applied sciences

MDPI

Communication

Thermal Hysteresis in Melting–Solidification of Nanoparticles

Victor M. Burlakov

Linacre College, University of Oxford, St. Cross Road, Oxford OX1 3JA, UK; victor.burlakov@linacre.ox.ac.uk

Abstract: The aim of this paper is the development of a qualitative understanding of thermal hysteresis, namely the difference between the melting T_m and solidification T_s temperatures of nanoparticles as a function of the particle size. In contrast to the melting temperature, the determination of the absolute value of the solidification temperature for nanoparticles is generally more difficult and subjected to significant uncertainties. In this study, we implemented a very generic approach based on classical nucleation theory and define the thermal hysteresis for a nanoparticle relative to its value for a much larger 'reference' particle made of the same material. The obtained thermal hysteresis is found to vanish when decreasing the nanoparticle size. The approach is illustrated using the examples of gold, bismuth, and platinum nanoparticles.

Keywords: nanoparticles; melting temperature; overcooling; thermal hysteresis

Citation: Burlakov, V.M. Thermal Hysteresis in Melting–Solidification of Nanoparticles. *Appl. Sci.* **2023**, *13*, 3809. https://doi.org/10.3390/app13063809

Academic Editors: Marilena Carbone and Alessandro Chiolerio

Received: 10 December 2022
Revised: 13 March 2023
Accepted: 14 March 2023
Published: 16 March 2023

1. Introduction

The melting of nanoparticles (NPs) has been widely studied both experimentally and theoretically [1–8]. It has been well established that the melting temperatures of NPs decrease when their size decreases, and this fact has been explained through a number of models (see the review presented in [9]). Almost all of these models approximate the particle shape using an ideal sphere with a radius R. The size-dependent melting temperature T_m can then be written in the generic form:

$$T_m = T_b \cdot \left(1 - \frac{X}{R}\right) \quad (1)$$

Where T_b is the melting temperature of the bulk, and the quantity X depends on the model. The simplest model is based on the condition for thermodynamic equilibrium at melting temperature T_m for the particle in solid (S) and liquid (L) states, which implies phase coexistence. Formally, this entails an equivalence of the corresponding atomic (molecular) chemical potentials $\mu_S = \mu_L$. The latter are determined from the corresponding free energies

$$F_S = \frac{4\pi}{3} {R_S}^3 n_S(-E_S - T \cdot S_S) + 4\pi R_S^2 \gamma_S, \quad F_L = \frac{4\pi}{3} R_L^3 n_L(-E_L - T \cdot S_L) + 4\pi R_L^2 \gamma_L \quad (2)$$

where $n_{S,L}$ are the atomic concentrations; $E_{S,L}$ and $S_{S,L}$ are the atomic cohesive energies and entropies, respectively; $\gamma_{S,L}$ are the surface energies of the corresponding states; and T is the temperature. At $T = T_m$, the condition $\mu_S = \mu_L$ results in

$$\Delta E - T_m \cdot \Delta S - \frac{2\Delta\gamma}{n_L R} = 0 \rightarrow T_m = \frac{\Delta E}{\Delta S}\left(1 - \frac{2\Delta\gamma}{\Delta E n_L R}\right) \quad (3)$$

where $R \equiv R_L$, $\Delta E = E_S - E_L$, $\Delta S = S_L - S_S$, and $\Delta\gamma = \gamma_S(n_L/n_S)^{2/3} - \gamma_L$. Assuming that the factor $\Delta E/\Delta S$ can be replaced with its asymptotic value at $R \rightarrow \infty$, namely, $\Delta E/\Delta S = T_b$, we obtain an expression similar to that given in Equation (1).

In contrast to melting, the solidification of particles is a highly non-equilibrium process initiated from a solid nucleus formed inside the particle bulk due to some degree of

fluctuation. Once the nucleus exceeds the critical size, it can grow further into the rest of the particle. Such a process is characterized by a certain energy barrier and can be described according to classical nucleation theory (CNT) [10,11]. The key parameter in the solidification process within the CNT is the nucleation probability

$$P(R, T_s) = N(R)M_0 \cdot \exp\left(-\frac{\Delta F_N(R, T_s)}{k_B T_s}\right) = \exp\left(-\frac{\Delta F_N(R, T_s)}{k_B T_s} + \ln(N(R) \cdot M_0)\right) \quad (4)$$

where $\Delta F_N(R, T_s)$ is the nucleation barrier, i.e., the free energy barrier for the formation of the critical solid nucleus inside the liquid particle of radius R, and k_B is the Boltzman factor. The factor $N(R) = 4/3 \cdot \pi R^3/v$ is the number of nucleation sites, while v is the characteristic volume of the nucleation site. The factor M_0 incorporates Zeldovich's factor and the attempt frequency to overcome the nucleation barrier and is assumed to be constant in the current context. The probabilistic nature of the solidification process results in a significant variation in the solidification temperature [12–17] and significantly hampers its theoretical predictions [18,19]. As a result, there is currently no clear picture of the size dependence of thermal hysteresis in nanoparticles.

This study presents an attempt to qualitatively understand the behavior of thermal hysteresis in the melting–solidification of NPs as a function of particle radius.

2. Results and Discussion

The probabilistic nature of material solidification means that the liquid-to-solid transformation is determined by the probability of forming a large enough (critical) solid nucleus inside the liquid bulk, which then grows further through the entire system (in our case, particles). Such a nucleation probability in the CNT is presented in Equation (4) and is proportional to the number of sites at which the nucleus can be formed (nucleation sites) and the frequency with which the nucleus at a given nucleation site is attempted to be generated. The probability of forming the critical nucleus in a single attempt is given by the Boltzmann-type exponential factor in Equation (4), wherein the activation energy is represented by the free energy difference (the nucleation barrier) between the two states of the particle: one containing the critical solid nucleus in the liquid particle, and the other is just the liquid particle. The nucleation barrier depends on several parameters, including the surface energy, which is different for liquid and solid particles; the solid–liquid interface energy; and the energy density freed upon solidification (heat of fusion).

In relation to the dependence on size, the solidification of particles is controlled by two factors: (i) the number of nucleation sites and (ii) the nucleation barrier. The size dependence of the former is relatively clear provided that the nucleation site's volume is independent of and small compared to the particle volume. In contrast, the size dependence of the nucleation barrier is less obvious, as illustrated by the analysis below.

2.1. Analysis of NP Solidification

The solidification processes in the NPs of different sizes can be analyzed within the CNT on the basis of an equal nucleation probability, i.e., $P(R, T) = Const$. This means that by choosing a reference particle of a radius R_0 and a solidification temperature T_{s0} and equating the nucleation probabilities

$$P(R, T_s) = P(R_0, T_{s0}) \quad (5)$$

we can express the solidification parameters for the NPs of a radius R in terms of those for the reference particle. The solidification of the NPs proceeds from the formation of a solid nucleus of a radius x. To implement Equation (2), we require a suitable expression for the nucleation barrier $\Delta F_N(R, T_s)$. As the surface energy for the solid state is always higher than that for the liquid state, we can assume that the solid nucleus is always surrounded by

liquid to minimize the energy of the particle. Assuming (for simplicity) that the nucleus is formed in the NP's center, the excess free energy associated with it takes the form

$$\Delta F_N\,(R, T_s, x) \approx \frac{4\pi}{3} x^3 n_S \left(-\Delta E + T_s \cdot \Delta S - \frac{\Delta n}{n_S} \frac{2\gamma_L}{3n_L R} \right) + 4\pi x^2 \gamma_{SL} \tag{6}$$

where γ_{SL} is the solid–liquid interface energy, $\Delta n = n_S - n_L$. The change in entropy upon melting ΔS as expressed using Equation (3) depends on the NP radius R; namely, it decreases when decreasing R. By substituting it into Equation (6), we obtain

$$\Delta F_N\,(R, T, x) \approx \frac{4\pi}{3} x^3 n_S \Delta E \left(-\delta \cdot \left(1 - \frac{\alpha}{R} \right) - \frac{\alpha}{R} \left(1 + \frac{\gamma_L}{\Delta\gamma} \frac{\Delta n}{n_S} \right) \right) + 4\pi x^2 \gamma_{SL} \tag{7}$$

where $\delta = 1 - T_s/T_m$, $\alpha = 2\Delta\gamma/(n_L \Delta E)$, and $\Delta n = n_S - n_L$. The parameter δ denotes relative thermal hysteresis for the NP. The nucleation barrier is defined as $\Delta F(R, T_s, x = x_{\mathrm{m}})$, where $x_m = 2\gamma_{SL} \cdot \left[n_S \Delta E \left(\delta \cdot \left(1 - \frac{\alpha}{R} \right) + \frac{\alpha}{R} \left(1 + \frac{\gamma_L}{\Delta\gamma} \frac{\Delta n}{n_S} \right) \right) \right]^{-1}$, and is equal to

$$\Delta F_N(R, T_s) \approx \frac{2\pi}{3} \frac{(2\gamma_{SL})^3}{(\Delta E)^2 n_S^2 \left(\delta \cdot \left(1 - \frac{\alpha}{R} \right) + \frac{\alpha}{R} \left(1 + \frac{\gamma_L}{\Delta\gamma} \frac{\Delta n}{n_S} \right) \right)^2} \tag{8}$$

It is worth pointing out that considering $0<\delta<< 1$, the nucleation barrier given by Equation (8) decreases with a decreasing particle radius.

To study the solidification of NPs as a function of their size, we use Equation (5) for the reference particle with the radius R_0, which is large enough that the terms $\sim 1/R_0$ in the corresponding nucleation barrier can be neglected. By substituting Equation (4) into Equation (5), for which $\Delta F_N(R, T_s)$ has been given by Equation (8), and omitting the terms that are identical for both actual and reference particles, we obtain

$$-\frac{4\pi}{3} \frac{\alpha^2 (1-\lambda)^2}{\beta(1-\delta) \cdot \left(\delta \cdot \left(1 - \frac{\alpha}{R} \right) + \frac{\alpha}{R}(1 + 6.7\lambda) \right)^2} + 3\ln(R) \approx -\frac{4\pi}{3} \frac{\alpha_0^2 (1-\lambda)^2}{\beta_0 (1-\delta_0) \delta_0^2} + 3\ln(R_0) \tag{9}$$

where $\beta = k_B T_m/\gamma_{SL}$, $\beta_0 = k_B T_{s0}/\gamma_{SL0}$, $\alpha_0 = 2\Delta\gamma_0/(n_L \Delta E_0)$, $\lambda = 1 - n_L/n_S$, and the parameters with '0' in the subscript correspond to the reference particle with the melting temperature T_{m0} and solidification temperature T_{s0}, i.e., for which relative thermal hysteresis $\delta_0 = 1 - T_{s0}/T_{m0}$. The logarithmic terms represent the R-dependent fractions of the nucleation sites' numbers. For illustrative purposes, in Equation (9), we also assumed that $\Delta\gamma \approx \gamma_{SL} \approx 0.15\gamma_L$ [20]. Besides the melting temperature for the NPs, the energy parameters ΔE, $\Delta\gamma$, and γ_{SL} also depend on the particle radius R. Some of their ratios, however, can be considered constants. For instance, a further simplification of Equation (9) can be performed if we define $\alpha \approx \alpha_0$ and $\beta \approx \beta_0$ [21,22]. Then, the ultimate equation for the relative thermal hysteresis δ reduces to

$$(1-\delta) \left(\delta \cdot \left(1 - \frac{\alpha_0}{R} \right) + \frac{\alpha_0}{R}(1 + 6.7\lambda) \right)^2 - \frac{(1-\delta_0)\delta_0^2}{1-B} \approx 0, \quad B = \frac{9(1-\delta_0)\delta_0^2 \beta_0}{4\pi\alpha_0^2 (1-\lambda)^2} \ln\left(\frac{R_0}{R} \right) \tag{10}$$

2.2. Thermal Hysteresis

The value of the parameter δ_0 can be defined as equal to that for the bulk; for most simple metals, it is close to 0.17 [12,13,23,24]. Notably, decreasing δ_0 to 0.1 (which is typical for a SnAgCu alloy [25]) does not change the qualitative behavior of δ as a function of R. To qualitatively understand the role of the parameters α_0 and β_0 in the present context of the relative thermal hysteresis, Equation (10) was solved numerically for $n_S \approx n_L = 40 \;\; nm^{-3}$, defining the reference particle radius as $R_0 = 50 \;\; \mu$. The results calculated for a number of α_0 and β_0 values are presented in Figure 1. According to the figure, the value of relative thermal hysteresis slightly increases when the particle radius decreases in the range of 50–0.5 μ. A similar trend was observed for the SnAgCu alloy when the particle size

decreased in the range of 500–100 μ [15]. In contrast, in the region of low R, the decrease in R results in a steep decrease in δ for all the parameter values analyzed herein. This thermal hysteresis behavior can be qualitatively explained by recalling that to maintain a constant nucleation probability (Equation (4)), the decrease in the number of nucleation sites (the term $3\ln(R)$ in Equation (9)) must be compensated for by the decrease in the nucleation barrier $\Delta F_N(R, T_s)$. To demonstrate the nucleation barrier can be decreased, it is convenient to represent $\Delta F_N(R, T_s)$ in Equation (9) for $\lambda \approx 0$ in the two extreme cases.

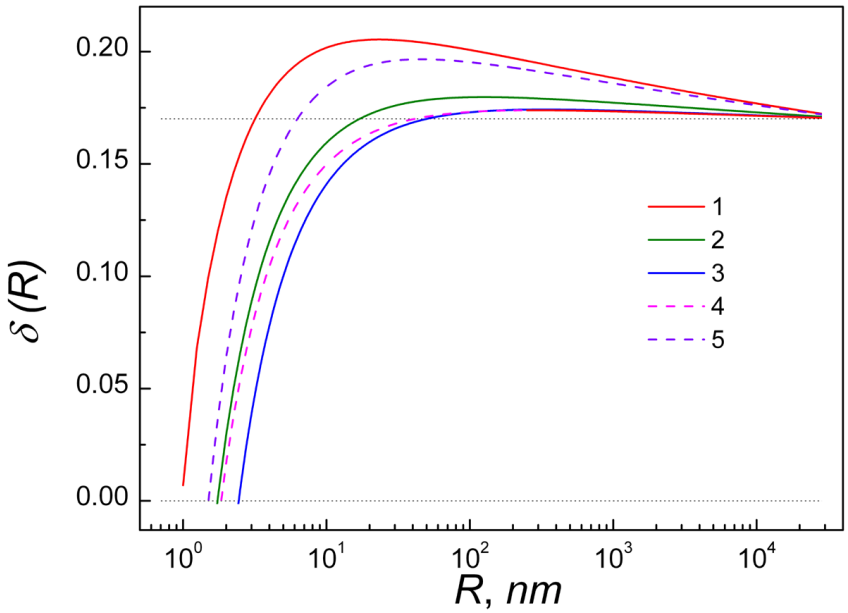

Figure 1. Relative thermal hysteresis as a function of the NP radius calculated by numerically solving Equation (10) for $\lambda = 0$ and for different values of α_0 $[nm]$ and $\beta_0[nm^2]$: 1—$\alpha_0 = 0.2$, $\beta_0 = 0.1$; 2—$\alpha_0 = 0.3$, $\beta_0 = 0.1$; 3—$\alpha_0 = 0.4$, $\beta_0 = 0.1$; 4—$\alpha_0 = 0.3$, $\beta_0 = 0.05$; 5—$\alpha_0 = 0.3$, $\beta_0 = 0.2$.

$$(i) \quad \Delta F_N(R, T_s) \approx \frac{4\pi}{3} \frac{{\alpha_0}^2}{\beta_0(1-\delta)\cdot\delta^2}, \quad R > 500 \ nm \tag{11}$$

$$(ii) \quad \Delta F_N(R, T_s) \approx \frac{4\pi}{3} \frac{{\alpha_0}^2}{\beta_0(1-\delta)\cdot\left(\delta\cdot\left(1-\frac{\alpha_0}{R}\right)+\frac{\alpha_0}{R}\right)^2}, \quad R < 10 \ nm \tag{12}$$

According to Equation (11), a decrease in $\Delta F_N(R, T_s)$ can be only achieved by increasing the value of δ. In the extreme case (*ii*), the logarithmic term in Equation (9) shows a very steep decrease when x increases (decreasing R). To compensate for this decrease, the corresponding nucleation barrier given by Equation (12) must also decrease by a commensurably steep decrease in δ.

To illustrate the relative thermal hysteresis behavior provided in Equation (10) with respect to real metals, we solved this equation for *Bi*, *Au*, and *Pt* NPs using available data for the latent heat of melting and surface energies [23,26,27]. According to Figure 2, a rather similar relative hysteresis behavior is observed for the *Pt* and *Au* particles, which show almost no increase at large particle sizes and a steep decrease to zero at R values of 2 and 3 nm, respectively.

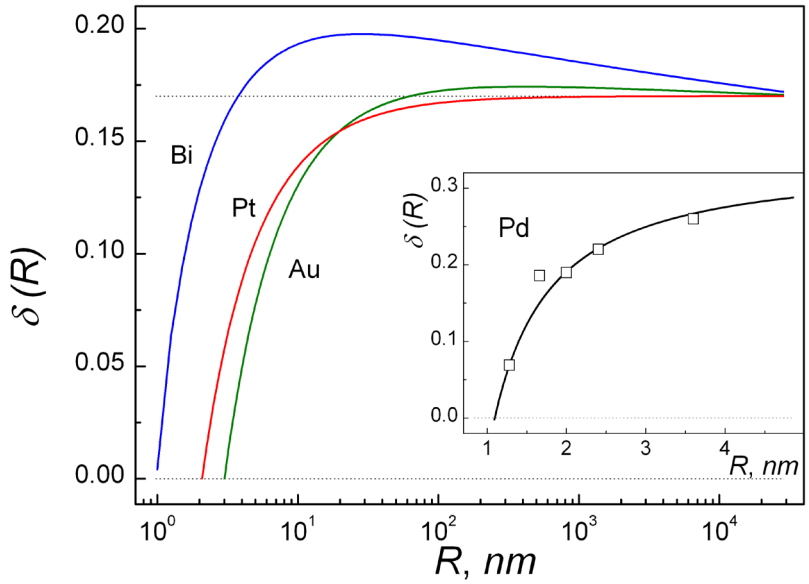

Figure 2. Relative thermal hysteresis as a function of the NP radius calculated by numerically solving Equation (10) for Bi: $\alpha_0 = 0.234$, $\beta_0 = 0.124$, $\lambda = -0.033$, Au: $\alpha_0 = 0.37$, $\beta_0 = 0.08$, $\lambda = 0.06$, Pt: $\alpha_0 = 0.29$, $\beta_0 = 0.087$, $\lambda = 0.02$. Insert: solid line denotes the solution from Equation (10) with respect to Palladium (Pd) with $\delta_0 = 0.28$, $\alpha_0 = 0.32$, $\beta_0 = 0.087$, $\lambda = 0$. Symbols are the results calculated using the values of melting and solidification temperatures for nanoparticles obtained by molecular dynamics simulations [28].

In contrast, the behavior of $\delta(R)$ for the Bi particles shows a noticeable increase with a decreasing R in the range of $R > 30$ nm and a steep decrease for smaller radii. Interestingly, the NP melting temperatures of the corresponding materials show a noticeable decrease in the same ranges of R values as those of δ. The available experimental data for thermal hysteresis in NPs are rather ambiguous, in some cases showing a significant decrease at low R values, which is in agreement with our numerical results [29]. A more quantitative verification of the proposed analytical approach can be performed by comparing its predictions with the results of numerical simulations, as illustrated in the insert in Figure 2 wherein Palladium is used as an example. As one can see, the relative hysteresis calculated using the simulated melting–solidification temperatures [28] (symbols) is quite closely approximated by the analytical curve obtained by solving Equation (10). Direct evidence of the decreased nucleation barrier, and hence thermal hysteresis for small NPs, can be found by observing the phase fluctuation in the Bi NPs under continuous electron beam illumination [16].

The presented analysis is based on several assumptions, which may restrict its applicability. The main assumption is that solidification can be described within a CNT for all particles in the size range of interest. An additional assumption about the nucleation probability is that the nucleation site volume v is independent of the particle size, which is true if the latter is large enough compared to v. Very little is known about the nucleation site volume in real systems. It is most likely that its size is of the order of a few interatomic distances, in which case the above assumptions seem to be realistic for nanoparticles with a radius over 1 nm. This can be applicable to particles made of pure metals and alloys provided that the alloy composition is homogeneous throughout the particles. Thus, we may conclude that the predicted size dependence of thermal hysteresis can be observed for particles made of these materials.

3. Conclusions

Using classical nucleation theory under the condition of the same nucleation probability for particles of different sizes, we analyzed relative thermal hysteresis $\delta = 1 - T_s/T_m$ with respect to the melting–solidification of particles. It has been found that δ exhibits

two trends upon decreasing the particle size: (i) a moderate increase for relatively large, greater-than-micron-sized particles, and (ii) a subsequent steep decrease for much smaller particles in the size range of nanometers. It has been shown that this trend (i) is due to a decrease in the number of nucleation sites upon decreasing the particle volume. The second trend (ii) is associated with the decrease in the nucleation barrier in the sufficiently small particles. Qualitatively, this latter decrease can be explained in terms of the increasing relative contribution of the surface energy to the entropy change associated with the particles' melting–solidification processes. Despite a rather simplified description of the particle solidification process, the obtained numerical results (in some cases) show a qualitative agreement with the available simulation data and experimental studies. The predicted decrease in thermal hysteresis in small nanoparticles can be interpreted in terms of a vanishing nucleation barrier, which may result in the random fluctuation of the particles between liquid and solid states. If experimentally realized for a large enough ensemble of similar nanoparticles, such an effect may be interesting for practical applications.

Funding: This research received no external funding.

Institutional Review Board Statement: Not applicable.

Informed Consent Statement: Not applicable.

Data Availability Statement: Data available in a publicly accessible repository.

Conflicts of Interest: The authors declare no conflict of interest.

References

1. Peppiatt, S.J. The melting of small particles. II. Bismuth. *Proc. R. Soc. London Ser. A Math. Phys. Sci.* **1975**, *345*, 401–412. [CrossRef]
2. Buffat, P.; Borel, J.-P. Size effect on the melting temperature of gold particles. *Phys. Rev. A* **1976**, *13*, 2287–2298. [CrossRef]
3. Allen, G.L.; Bayles, R.A.; Gile, W.W.; Jesser, W.A. Small particle melting of pure metals. *Thin Solid Film.* **1986**, *144*, 297–308. [CrossRef]
4. Kellermann, G.; Pereira, F.L.C.; Craievich, A.F. Determination of the melting temperature of spherical nanoparticles in dilute solution as a function of their radius by exclusively using the small-angle X-ray scattering technique. *J. Appl. Cryst.* **2020**, *53*, 455–463. [CrossRef]
5. Chang, J.; Johnson, E. Surface and bulk melting of small metal clusters. *Philos. Mag.* **2005**, *85*, 3617–3627. [CrossRef]
6. Garrigos, R.; Cheyssac, P.; Kofman, R. Melting for lead particles of very small sizes; influence of surface phenomena. *Z. Phys. D At. Mol. Clust.* **1989**, *12*, 497–500. [CrossRef]
7. Schlexer, P.; Andersen, A.B.; Sebok, B.; Chorkendorff, I.; Schiøtz, J.; Hansen, T.W. Size-Dependence of the Melting Temperature of Individual Au Nanoparticles. *Part. Part. Syst. Charact.* **2019**, *36*, 1800480. [CrossRef]
8. Goldstein, A.N.; Echer, C.M.; Alivisatos, A.P. Melting in Semiconductor Nanocrystals. *Science* **1992**, *256*, 1425–1427. [CrossRef]
9. Guenther, G.; Guillon, O. Models of size-dependent nanoparticle melting tested on gold. *J. Mater. Sci.* **2014**, *49*, 7915–7932. [CrossRef]
10. Sear, R.P. Nucleation: Theory and applications to protein solutions and colloidal suspensions. *J. Phys. Condens. Matter.* **2007**, *19*, 033101. [CrossRef]
11. Oxtoby, D.W. Homogeneous nucleation: Theory and experiment. *J. Phys. Condens. Matter* **1992**, *4*, 7627–7650. [CrossRef]
12. Turnbull, D.; Cech, R.E. Microscopic Observation of the Solidification of Small Metal Droplets. *J. Appl. Phys.* **1950**, *21*, 804. [CrossRef]
13. Turnbull, D. Formation of Crystal Nuclei in Liquid Metals. *J. Appl. Phys.* **1950**, *21*, 1022–1027. [CrossRef]
14. Simon, C.; Peterlechner, M.; Wilde, G. Experimental determination of the nucleation rates of undercooled micron-sized liquid droplets based on fast chip calorimetry. *Thermochim. Acta* **2015**, *603*, 39–45. [CrossRef]
15. Kinyanjui, R.; Lehman, L.P.; Zavalij, L.; Cotts, E. Effect of sample size on the solidification temperature and microstructure of SnAgCu near eutectic alloys. *J. Mater. Res.* **2005**, *20*, 2914–2918. [CrossRef]
16. Li, Y.; Zang, L.; Jacobs, D.L.; Zhao, J.; Yue, X.; Wang, C. In situ study on atomic mechanism of melting and freezing of single bismuth nanoparticles. *Nat. Commun.* **2017**, *8*, 14462. [CrossRef]
17. Shibuta, Y.; Suzuki, T. Melting and solidification point of fcc-metal nanoparticles with respect to particle size: A molecular dynamics study. *Chem. Phys. Lett.* **2010**, *498*, 323–327. [CrossRef]
18. Kalyanaraman, R. Nucleation energetics during homogeneous solidification in elemental metallic liquids. *J. Appl. Phys.* **2008**, *104*, 033506. [CrossRef]
19. Vekilov, P.G. Nucleation. *Cryst. Growth Des.* **2010**, *10*, 5007–5019. [CrossRef] [PubMed]
20. Skapski, A.S. A Theory of Surface Tension of Solids—I. *Acta Metall.* **1956**, *4*, 576–582. [CrossRef]

21. Ouyang, G.; Tan, X.; Yang, G. Thermodynamic model of the surface energy of nanocrystals. *Phys. Rev. B* **2006**, *74*, 195408. [CrossRef]
22. Jiang, X.; Xiao, B.; Lan, R.; Gu, X.; Zhang, X.; Sheng, H. Estimation of the solid-liquid interface energy for metal elements. *Comput. Mater. Sci.* **2019**, *170*, 109174. [CrossRef]
23. Jian, Z.; Kuribayashi, K.; Jie, W. Solid-liquid Interface Energy of Metals at Melting Point and Undercooled State. *Mater. Trans.* **2002**, *43*, 721–726. [CrossRef]
24. Flemings, M.C.; Shiohara, Y. Solidification of Undercooled Metals. *Mater. Sci. Eng.* **1984**, *65*, 157–170. [CrossRef]
25. Rudajevová, A.; Dušek, K. Influence of the thermal history and composition on the melting/solidification process in Sn-Ag-Cu solders. *Kov. Mater.* **2012**, *50*, 295–300. [CrossRef]
26. Vitos, L.; Ruban, A.V.; Skriver, H.L.; Kollar, J. The surface energy of metals. *Surf. Sci.* **1998**, *411*, 186–202. [CrossRef]
27. Zhang, S. The solid–liquid interface energy at the melting temperature of metal materials. *Nanomater. Energy* **2019**, *8*, 107–113. [CrossRef]
28. Hou, M. Solid–liquid and liquid–solid transitions in metal nanoparticles. *Phys. Chem. Chem. Phys.* **2017**, *19*, 5994–6005. [CrossRef] [PubMed]
29. Zhdanov, V.P.; Schwind, M.; Zoric, I.; Kasemo, B. Overheating and undercooling during melting and crystallization of metal nanoparticles. *Physica E* **2010**, *42*, 1990–1994. [CrossRef]